

Topology of circular orbits of charged particles in black holes with multiple horizons

Yong Song^{a*}, Jia Li^{a†}, Yiting Cen^{a‡}, Kai Diao^{b§}, Xiaofeng Zhao^{a¶}, and Shunping Shi^{a**}

^a College of Physics, Chengdu University of Technology, Chengdu, Sichuan 610059, China,

^b Yin bin Campus, Chengdu Technological University Yinbin, 644000 Sichuan, China

(Dated: April 8, 2025)

The study of the topological properties of circular orbits is opening up new perspectives for exploring the spacetime structure around black holes. In this work, we investigate how the charged properties of particles affect the topological characteristics of circular orbits for charged test particles in asymptotically flat, AdS, and dS black holes. Our findings demonstrate that the charged properties not only influence the topological properties of timelike circular orbits but also impact those of null circular orbits. Additionally, we explore scenarios involving multiple horizons and find that for a multi-horizon black hole, if a circular orbit can exist between two neighboring horizons, there will always be both a null circular orbit and a timelike circular orbit. Whether these orbits are stable or unstable depends on the potential function.

I. INTRODUCTION

Circular orbits in spacetime are crucial for understanding the properties and behaviors of black holes. These orbits provide key insights into black hole gravitational fields and related phenomena. In recent years, methods based on topological theory have been developed to study the properties of circular orbits. This approach offers a novel framework for analyzing the existence and stability of such orbits. It not only enhances our comprehension of the spacetime structure around black holes, but also opens up promising new research directions for the future.

In 2017, Cunha, Berti, and Herdeiro introduced a novel topological approach, which, without relying on specific field equations, studies the photon sphere (PS) or light ring (LR) stability for ultra-compact objects [1]. Using the Brouwer degree of a continuous map, they found that the LRs of compact objects always come in pairs. Though this result is generally valid, an important exception arises when degenerate light rings are present [2]. Further, Cunha and Herdeiro advanced the study by generalizing it to a four-dimensional stationary, axisymmetric, asymptotically flat black hole spacetime [3]. They proved that at least one standard LR (i.e., an unstable LR) exists outside the black hole horizon for each rotation sense by calculating the winding number of the vector field defined by an effective potential on the orthogonal (r, θ) -space. Moreover, following their topological argument, horizonless ultra-compact objects like boson stars exhibit an even number of non-degenerate LRs. Inspired by the work of Cunha et al., Wei, based on Duan's topological current ϕ -mapping theory [4, 5], computed the topological charge for a black hole with asymptotically flat, AdS, and dS behaviors of the boundary [6]. They found that all these black holes admit a minus one topological charge, indicating the existence of at least one standard PS. They also found that Duan's topological current ϕ -mapping can be used for the study of black hole thermodynamics, providing new insights into this field [7, 8].

Previous studies have focused on null circular orbits, while the case for timelike circular orbits (TCOs) is a bit more complicated. There have been several studies on the topological properties of TCOs [9–11]. The main conclusions are that, for a generic black hole spacetime, TCOs with fixed angular momentum always come in pairs, with one being stable and the other being unstable. A positive or negative winding number corresponds to a stable or unstable TCO, respectively. This result is universal and is independent of the angular momentum of the particle and the black hole parameters. In 2024, Xu and Wei studied the topological phenomena of TCOs for charged test particles in asymptotically flat black holes and found that the charge-to-mass ratio (specific charge) influences the topological behavior of TCOs [12].

While research on the topological properties of circular orbits has made progress, several questions remain. For example: What about the topological properties of circular orbits between neighboring horizons if there are multiple horizons? The charge of a particle affects the topological properties of TCOs, so does it also affect the properties of null circular orbits? Moreover, Do the different asymptotic behaviors of black holes have any impact on the topological properties of circular orbits of charged particles? If so, what are the specific effects? These questions are worthy of in-depth study. In this work, we will investigate the topological properties of circular orbits of charged particles in asymptotically flat, anti-de Sitter (AdS), and de Sitter (dS) black holes with multiple horizons. We find that the charged property not only have effect on the topological properties of timelike circular orbits, but also impact those of null circular orbits. Additionally, for a multi-horizon black hole, if there exists a circular orbit between two neighboring horizons, then there always exists a null circular orbit and a timelike circular orbit, whether they are stable or unstable depends on the potential function.

* e-mail address: syong@cdut.edu.cn

† e-mail address: lijia@cdut.edu.cn (corresponding author)

‡ e-mail address: 2199882193@qq.com

§ e-mail address: kai_diao@qq.com

¶ e-mail address: 59403804@qq.com

** e-mail address: shishunping13@cdut.edu.cn

The present paper is organized as follows. In Sec. II, we will review the charged black hole and the topological approach for circular orbits. In Sec. III, we will study the topology of circular orbits of charged particles between two neighboring horizons. In Sec. IV, we will study the topology of circular orbits of charged particles in asymptotically flat, AdS, and dS black holes. In Sec. V, we summarize and discuss our results. In Appendix. A, we present the results on the topological properties of circular orbits in the case of $V = V_-$.

II. TOPOLOGICAL APPROACH FOR CIRCULAR ORBITS

In a charged black hole background, the line element in standard spherical coordinates ($x = t, r, \theta, \phi$) can be written as [13]

$$ds^2 = -f(r)dt^2 + \frac{1}{g(r)}dr^2 + h(r)(d\theta^2 + \sin^2\theta d\phi^2), \quad (2.1)$$

where $f(r)$, $g(r)$ and $h(r)$ are functions that depend only on the radial coordinate r , and the horizon is defined by $f(r_h) = 0$. A Maxwell field

$$A = A_\mu dx^\mu, \quad \text{and} \quad A_\mu = (A_t(r), 0, 0, 0). \quad (2.2)$$

is assumed to exist, and A_μ are the components of the electromagnetic 4-potential. At infinity, we assume $A_t(r)$ has the following asymptotic behavior

$$A_t(r \rightarrow \infty) \sim -\frac{Q}{r}. \quad (2.3)$$

where Q is the charge of the black hole. The motion of a test particle with charge q and mass μ moving in the background (2.1) is described by the following Lagrangian density [14–16]:

$$\begin{aligned} \mathcal{L} &= \frac{1}{2}g_{\alpha\beta}\dot{x}^\alpha\dot{x}^\beta + \epsilon A_\alpha\dot{x}^\alpha, \\ &= \frac{1}{2}\left[-f\dot{t}^2 + \frac{\dot{r}^2}{g} + h(\dot{\theta}^2 + \sin^2\theta\dot{\phi}^2)\right] + \epsilon A_t\dot{t}, \end{aligned} \quad (2.4)$$

where the dot represents differentiation with respect to the proper time, and the parameter $\epsilon = \frac{q}{\mu}$ is the specific charge of the test particle.

Since the Lagrangian density (2.4) does not depend explicitly on the variables t and ϕ , the following two conserved quantities exist

$$p_t \equiv \frac{\partial\mathcal{L}}{\partial\dot{t}} = -\left(f\dot{t} - \epsilon A_t\right) = -E, \quad (2.5)$$

$$p_\phi = \frac{\partial\mathcal{L}}{\partial\dot{\phi}} = h\sin^2\theta\dot{\phi} = L, \quad (2.6)$$

where E and L are the specific energy and angular momentum of the particles, respectively. In the spherically symmetric case, L can always be chosen to be greater than zero, i.e., $L > 0$. From the normalization of the four-velocity (\dot{x}^μ), we have

$$g_{\mu\nu}\dot{x}^\mu\dot{x}^\nu = -\mu^2, \quad (2.7)$$

where $\mu^2 = 1, 0, -1$ correspond to the timelike, null, and spacelike geodesics, respectively. Considering the metric (2.1), one can obtain

$$-f\dot{t}^2 + \frac{\dot{r}^2}{g} + h\dot{\theta}^2 + h\sin^2\theta\dot{\phi}^2 + \mu^2 = 0. \quad (2.8)$$

and the kinetic term \mathcal{K} and the potential term \mathcal{V} can be defined as

$$\mathcal{K} = \frac{\dot{r}^2}{g} + h\dot{\theta}^2, \quad (2.9)$$

$$\mathcal{V} = -f\dot{t}^2 + h\sin^2\theta\dot{\phi}^2 + \mu^2. \quad (2.10)$$

Therefore, the motion of the test particle (2.8) becomes

$$\mathcal{K} + \mathcal{V} = 0. \quad (2.11)$$

Note that the kinetic term $\mathcal{K} \geq 0$, and the inequality is only saturated when $\dot{r} = \dot{\theta} = 0$. The motion of the particles can be completely governed by the effective potential \mathcal{V} .

Considering Eqs.(2.5) and (2.6), the potential (2.10) can be reduced to

$$\mathcal{V} = -\frac{1}{f}(E - V_+)(E - V_-), \quad (2.12)$$

where

$$V_{\pm} = -\epsilon A_t \pm \sqrt{f\left(\mu^2 + \frac{L^2}{h \sin^2 \theta}\right)}, \quad (2.13)$$

The circular motion of the charged particles can be described using the following equations:

$$\partial_{\mu} V_{\pm} = 0, \quad V_{\pm} = E. \quad (2.14)$$

It should be noted that $\partial_{\mu} V_{\pm}$ here not only depends on r and the specific angular momentum L , but also on the specific charge ϵ of the test particle.

In order to give a global topology, we require that the values of the specific angular momentum and the specific charge do not change the asymptotic behavior of $\partial_r V_{\pm}$ at the boundary of the (r, θ) plane. Here we only consider the case of $V = V_+$. For $V = V_-$, one can see the results in Appendix A. Following ref. [6], we define a vector field $\phi = (\phi^r, \phi^{\theta})$

$$\phi^r = \frac{\partial_r V}{\sqrt{g_{rr}}}, \quad \phi^{\theta} = \frac{\partial_{\theta} V}{\sqrt{g_{\theta\theta}}}, \quad (2.15)$$

in a flat vector space. For a charged massless particle, we have $\mu^2 = 0$. From Eqs.(2.13) and (2.15), one can get

$$\phi^r = -\epsilon A'_t \sqrt{g} + \frac{L(hf' - fh')}{2h^{3/2} \sin \theta} \sqrt{\frac{g}{f}}, \quad (2.16)$$

$$\phi^{\theta} = -\frac{\sqrt{f} L \cos \theta}{h \sin^2 \theta}. \quad (2.17)$$

For a charged massive particle, we have $\mu^2 = 1$. Then, one obtains

$$\phi^r = -\epsilon A'_t \sqrt{g} + \frac{f' h^2 \sin^2 \theta + L^2(hf' - fh')}{2h^{3/2} \sin \theta \sqrt{h \sin^2 \theta + L^2}} \sqrt{\frac{g}{f}}, \quad (2.18)$$

$$\phi^{\theta} = -\frac{\sqrt{f} L^2 \cos \theta}{h \sin^2 \theta \sqrt{h \sin^2 \theta + L^2}}. \quad (2.19)$$

It follows that $\partial^{\mu} V_{\pm} \partial_{\mu} V_{\pm} = (\phi^r)^2 + (\phi^{\theta})^2 = \|\phi\|^2$, where $\|\phi\| = \sqrt{\phi^a \phi_a}$. Hence, in terms of the vector field ϕ^a , $\phi^a = 0 \Leftrightarrow \|\phi\| = 0$. Obviously, $\phi^a = 0$ corresponds to the circular orbits of charged particles and $\theta = \pi/2$ as expected. Define an angle Ω such that $\phi^r = \phi \cos \Omega$, $\phi^{\theta} = \phi \sin \Omega$, and $\Omega = \arctan(\phi^{\theta}/\phi^r)$.

For each circular orbit, one can assign a topological charge. From [4–6], the topological current linked to the topological charge is as follows:

$$j^{\mu} = \frac{1}{2\pi} \epsilon^{\mu\nu\rho} \epsilon_{ab} \partial_{\nu} n^a \partial_{\rho} n^b, \quad (2.20)$$

here, $x^{\mu} = (t, r, \theta)$ and the unit vector $n^a = (n^r, n^{\theta}) = (\phi^r/\|\phi\|, \phi^{\theta}/\|\phi\|)$. This current is conserved and can be further simplified to

$$j^{\mu} = \delta^2(\phi) J^{\mu} \left(\frac{\phi}{x} \right) \quad (2.21)$$

with the Jacobi tensor given by $\epsilon^{ab} J^{\mu} \left(\frac{\phi}{x} \right) = \epsilon^{\mu\nu\rho} \partial_{\nu} \phi^a \partial_{\rho} \phi^b$. It is noteworthy that J^{μ} only has nonzero values at the zero points of the vector ϕ . The density of the topological current is obtained by denoting the i -th zero point as $\vec{x} - \vec{z}_i$.

$$j^0 = \sum_i^N = \beta_i \eta_i \delta^2(\vec{x} - \vec{z}_i), \quad (2.22)$$

where the Hopf index (β_i) and the Brouwer degree (η_i) of the i -th zero point are expressed. The topological number is obtained by integrating the density of the topological current over the given region Σ

$$W = \int_{\Sigma} j^0 d^2x = \sum_i^N \beta_i \eta_i = \sum_i^N w_i, \quad (2.23)$$

The symbol w_i signifies the winding number associated with the i -th zero point of the vector field ϕ enclosed within the region Σ . The topological number can be determined by evaluating the change in direction, denoted as Ω , of the vector as it traverses a counterclockwise closed path $I = \partial\Sigma$

$$W = \frac{1}{2\pi} \oint_I d\Omega. \quad (2.24)$$

Below, we choose the contour $C = \sum_i \cup l_i$ which encloses Σ , as shown in Fig. 1.

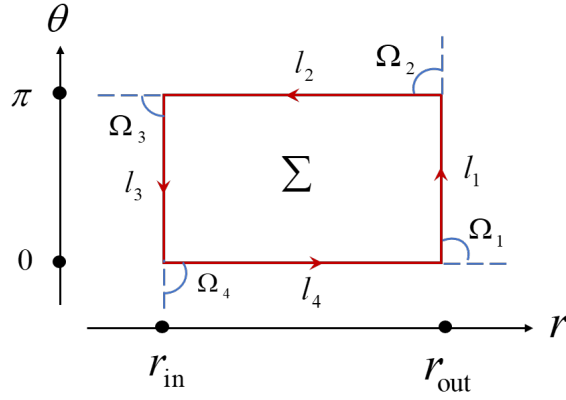


FIG. 1: Representation of the contour $C = \sum_i \cup l_i$ (which encloses Σ) on the (r, θ) plane. The curve C has a positive orientation, marked with the red arrows. r_{in} and r_{out} have different meanings in different cases. The angle Ω_i represents the change in direction of the vector ϕ^a at the joint of two l_i .

III. BETWEEN TWO NEIGHBORING HORIZONS

In this section, we study the topology of the circular orbits of charged particles between two neighboring horizons.

Assume that there are multiple horizons and consider two neighboring horizons r_{h_1} and r_{h_2} with $r_{h_1} < r_{h_2}$. The behavior of $f(r)$ is given in Fig. 2. Below, we only consider the situation (a) in Fig. 2. For the situation (b), since $f(r) < 0$ between r_{h_1} and r_{h_2} would lead to ϕ^θ and ϕ^r being undefined, the circular orbit in this case is forbidden. At the horizon, one has $f(r_h) = g(r_h) = 0$, while $\sqrt{g/f}|_{r_h}$ remains finite.

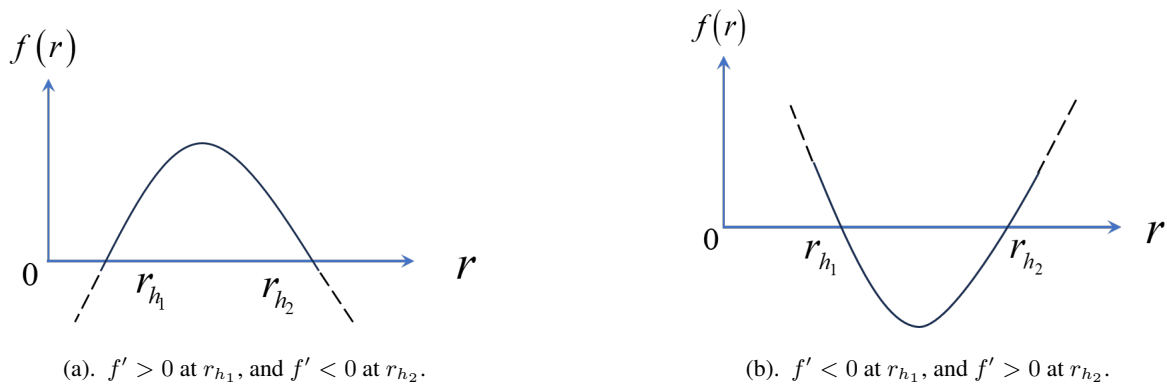


FIG. 2: The behavior of $f(r)$ in the region between two neighboring horizons.

A. charged massless particles

In this subsection, we study the topology of null circular orbits of charged massless particles between r_{h_1} and r_{h_2} . To calculate Q , one needs to study the boundary behaviors of Eqs.(2.16) and (2.17).

Here, we adopt the contour C defined in [3, 6], where $C = \sum_i l_i$ or the union of four line segments $l_1 \sim l_4: \{r_{\text{out}} = r_{h_2}, 0 \leq \theta \leq \pi\} \cup \{\theta = \pi, r_{h_1} \leq r < r_{h_2}\} \cup \{r_{\text{in}} = r_{h_1}, 0 \leq \theta \leq \pi\} \cup \{\theta = 0, r_{h_1} \leq r < r_{h_2}\}$.

Referring to [6], we study the asymptotic behavior of Eqs. (2.16) and (2.17). At r_{h_1} , we have

$$\phi_{l_3}^r(r \rightarrow r_{h_1}^+) > 0, \quad \phi_{l_3}^\theta(r \rightarrow r_{h_1}^+) \rightarrow 0, \quad (3.1)$$

where $f'(r_{h_1}) > 0$ is used. The vector ϕ is horizontal and points to the left at the horizon r_{h_1} , and thus $\Omega_{l_3} = 0$.

At r_{h_2} , we have

$$\phi_{l_1}^r(r \rightarrow r_{h_2}^-) < 0, \quad \phi_{l_1}^\theta(r \rightarrow r_{h_2}^-) \rightarrow 0, \quad (3.2)$$

where $f'(r_{h_2}) < 0$ is used. The vector ϕ is horizontal and points to the right at the horizon r_{h_2} , and thus $\Omega_{l_1} = \pi$ or $-\pi$.

At $\theta = 0$ and π , we have, respectively,

$$\phi_{l_4}^r(\theta \rightarrow 0^+) \sim \frac{1}{\theta}, \quad \phi_{l_4}^\theta(\theta \rightarrow 0^+) \sim -\frac{1}{\theta^2}, \quad \phi_{l_2}^r(\theta \rightarrow \pi^-) \sim \frac{1}{\pi - \theta}, \quad \phi_{l_2}^\theta(\theta \rightarrow \pi^-) \sim \frac{1}{(\pi - \theta)^2}, \quad (3.3)$$

So, we have $\Omega_{l_2} = \frac{\pi}{2}$ and $\Omega_{l_4} = -\frac{\pi}{2}$.

From the above, we conclude that $\Delta\Omega_1 = \Delta\Omega_2 = \Delta\Omega_3 = \Delta\Omega_4 = 0$ and $\Omega_1 = \Omega_2 = \Omega_3 = \Omega_4 = -\frac{\pi}{2}$. Therefore, we can obtain

$$W = \frac{1}{2\pi}(\Delta\Omega_{l_1} + \Delta\Omega_{l_2} + \Delta\Omega_{l_3} + \Delta\Omega_{l_4} + \Omega_1 + \Omega_2 + \Omega_3 + \Omega_4) = -1. \quad (3.4)$$

Based on the results in [3, 9], $W = 1$ indicates that there exists at least one stable circular orbit in the region under study, whereas $W = -1$ indicates that there exists at least one unstable circular orbit in the region under study. In our case, there is always at least one unstable null circular orbit between r_{h_1} and r_{h_2} .

B. charged massive particles

In this subsection, we study the topology of charged massive circular orbits between r_{h_1} and r_{h_2} . To do this, we need to examine the boundary behaviors of Eqs. (2.18) and (2.19). By following the steps outlined above, we can easily obtain the results for situation (a) in Fig. 2.

$$W = -1. \quad (3.5)$$

Summary of this section: Independent of the asymptotic behavior of black holes and the charge of particles, for two neighboring horizons, if there exist circular orbits, then there exists at least one null unstable circular orbit and one unstable timelike circular orbit.

IV. OUTSIDER THE OUTERMOST HORIZON

A. Asymptotically flat black holes

In an asymptotically flat black hole, the contour $C = \sum_i l_i$ can be defined as: $\{r_{\text{out}} = \infty, 0 \leq \theta \leq \pi\} \cup \{\theta = \pi, r_h \leq r < \infty\} \cup \{r_{\text{in}} = r_h, 0 \leq \theta \leq \pi\} \cup \{\theta = 0, r_h \leq r < \infty\}$. It should be noted that here r_h represents the outermost horizon.

In an asymptotically flat black hole with the solution described by (2.1), the metric functions exhibit the following asymptotic behaviors at $r \rightarrow \infty$:

$$f \sim 1 - \frac{2M}{r} + \mathcal{O}\left(\frac{1}{r^2}\right), \quad g \sim 1 - \frac{2M}{r} + \mathcal{O}\left(\frac{1}{r^2}\right), \quad h \sim r^2. \quad (4.1)$$

where M is the black hole mass, which is always positive. For $r_h < r < \infty$, $f(r)$ behaves as shown in Fig. (3), and $f'(r) > 0$ at r_h .

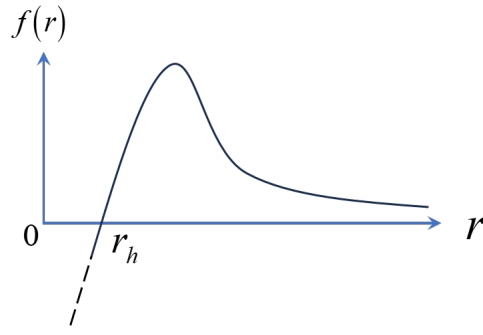


FIG. 3: The behavior of $f(r)$ in an asymptotically flat black hole. At r_h , one has $f'(r) > 0$.

The contour we have chosen in asymptotically flat spacetimes is shown in Fig. 4.

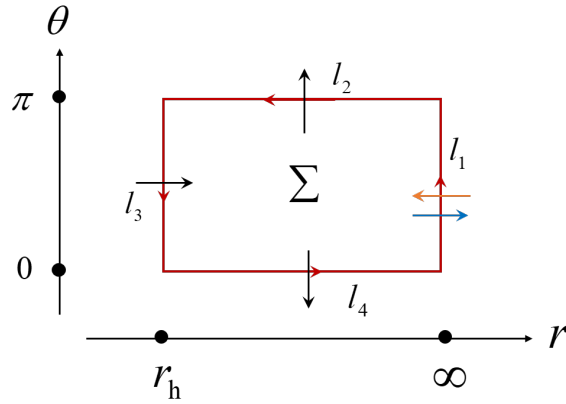


FIG. 4: Representation of the contour $C = \sum_i l_i$ (which encloses Σ) on the (r, θ) plane. The curve C has a positive orientation, marked with the red arrows. The black, blue and yellow arrows indicate the approximate directions of the vector ϕ at the boundaries.

1. charged massless particles

At the horizon, from Eqs.(2.16) and (2.17), we obtain

$$\phi_{l_3}^r(r \rightarrow r_h^+) > 0, \quad \phi_{l_3}^\theta(r \rightarrow r_h^+) \rightarrow 0, \quad (4.2)$$

where we have used the fact that $f'(r_h) > 0$. Consequently, the vector ϕ is oriented horizontally to the right at the horizon, which implies $\Omega_{l_3} = 0$. At $\theta = 0$ and π , the results are consistent with those in the previous section.

Lastly, let us consider Ω along l_1 . When $r \rightarrow \infty$,

$$\phi_{l_1}^r(r \rightarrow \infty) \sim -\frac{\epsilon Q + L}{r^2} + \frac{3ML}{r^3} \quad (4.3)$$

on the equatorial plane. If $-\epsilon Q < L$, then $\phi_{l_1}^r(r \rightarrow \infty) \sim -\frac{\epsilon Q + L}{r^2} < 0$. As a result, by ignoring the specific value of ϕ^θ , the direction of the vector ϕ is to the left. As shown in Fig. 4, the direction of the vector is outward at $\theta = 0$ and π , and to the right at $r = r_h$, and to the left at ∞ (denoted by a yellow arrow), ignoring any possible inclination. According to the asymptotic behaviors of ϕ , one can easily obtain

$$W = \frac{1}{2\pi} \oint d\Omega = \frac{1}{2\pi} \times (-2\pi) = -1, \quad (4.4)$$

which means that there will always be at least one unstable null circular orbit outside the event horizon in an asymptotically flat black hole.

If $-\epsilon Q \geq L$, then $\phi_{l_1}^r(r \rightarrow \infty) > 0$, and the direction of the vector ϕ is to the right at ∞ (denoted by a blue arrow in Fig. 4), ignoring any possible inclination. According to the asymptotic behaviors of ϕ , one can easily get

$$W = \frac{1}{2\pi} \oint d\Omega = \frac{1}{2\pi} \times (-\pi) + \frac{1}{2\pi} \times (\pi) = 0, \quad (4.5)$$

which means that if null circular orbits exist in asymptotically flat black holes, they must occur in pairs, with one being stable and the other being unstable.

2. charged massive particles

At the horizon, it is easy to obtain

$$\phi_{l_3}^r(r \rightarrow r_h^+) > 0, \quad \phi_{l_3}^\theta(r \rightarrow r_h^+) \rightarrow 0, \quad (4.6)$$

where $f'(r_h) > 0$ is used. Consequently, the vector ϕ is oriented horizontally to the right at the horizon, which implies $\Omega_{l_3} = 0$. At $\theta = 0$ and π , we respectively have

$$\phi_{l_4}^r(\theta \rightarrow 0^+) \sim \frac{1}{\theta}, \quad \phi_{l_4}^\theta(\theta \rightarrow 0^+) \sim -\frac{1}{\theta^2}, \quad \phi_{l_2}^r(\theta \rightarrow \pi^-) \sim \frac{1}{\pi - \theta}, \quad \phi_{l_2}^\theta(\theta \rightarrow \pi^-) \sim \frac{1}{(\pi - \theta)^2}, \quad (4.7)$$

Thus, we have $\Omega_{l_2} = \frac{\pi}{2}$ and $\Omega_{l_4} = -\frac{\pi}{2}$.

Lastly, let us consider Ω along l_1 . At $r \rightarrow \infty$, one have

$$\phi_{l_1}^r(r \rightarrow \infty) \sim \frac{M - \epsilon Q}{r^2} - \frac{L^2}{r^3} \quad (4.8)$$

on the equatorial plane. If $M > \epsilon Q$, $\phi_{l_1}^r(r \rightarrow \infty) \sim \frac{M - \epsilon Q}{r^2} > 0$, and the direction of the vector ϕ is to the right at ∞ (denoted by a blue arrow in Fig.4), ignoring any possible inclination. According to the asymptotic behaviors of ϕ , one can easily get

$$W = \frac{1}{2\pi} \oint d\Omega = \frac{1}{2\pi} \times (-\pi) + \frac{1}{2\pi} \times (\pi) = 0, \quad (4.9)$$

which means that if TCOs exist outside the outermost horizon in asymptotically flat spacetime, they must occur in pairs, with one being stable and the other being unstable.

If $M \leq \epsilon Q$, $\phi_{l_1}^r(r \rightarrow \infty) < 0$, and the direction of the vector ϕ is to the left at ∞ (denoted by a black arrow in Fig.4), ignoring any possible inclination. According to the asymptotic behaviors of ϕ , one can easily get

$$W = \frac{1}{2\pi} \oint d\Omega = \frac{1}{2\pi} \times (-\pi) + \frac{1}{2\pi} \times (-\pi) = -1, \quad (4.10)$$

which means that there will always be at least one unstable TCO outside the event horizon in an asymptotically flat black hole. These results are consistent with those in Ref. [12]. Here, we further consider the case that they did not address, namely the case where $M = \epsilon Q$.

3. RN black hole

We use Reissner-Nordström (RN) black holes as an example to verify the previous conclusions. Consider a non-extreme RN black hole, where the functions $f(r)$, $g(r)$ and $h(r)$ in (2.1) are

$$f(r) = g(r) = 1 - \frac{2M}{r} + \frac{Q^2}{r^2}, \quad h(r) = r^2. \quad (4.11)$$

Here, $M > Q$. There are two horizons r_- and r_+ , defined by $f(r_-) = f(r_+) = 0$, and

$$r_{\pm} = M \pm \sqrt{M^2 - Q^2}. \quad (4.12)$$

The associated electromagnetic potential is

$$A = -\frac{Q}{r} dt. \quad (4.13)$$

Below, we set $M = 1$ and $Q = 0.6$. The graph of the function $f(r)$ is shown in Fig. 5, with $r_- = 0.2$, $r_+ = 1.8$.

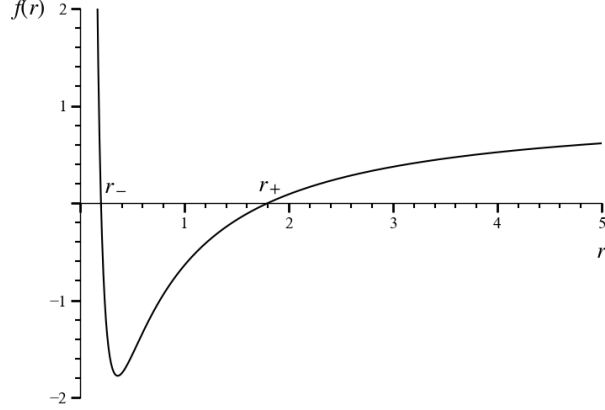


FIG. 5: The behavior of $f(r)$ in RN black hole. At r_- , one has $f'(r) < 0$; at r_+ , one has $f'(r) < 0$.

For the region r_- to r_+ , there are no circular orbits. Therefore, we focus on the case where $r > r_+$. By analyzing the graph of the potential function, we can determine whether circular orbits exist and assess their stability. In the following analysis, we will concentrate on the graphical representation of the potential function. The number of extrema on the graph corresponds to the number of circular orbits. Specifically, a local maximum on the graph signifies an unstable circular orbit, while a local minimum indicates a stable circular orbit.

Due to the spherical symmetry of the system, we can study the circular motion of a charged particle confined to the equatorial plane. From equation (2.13), we derive the effective potential of the particle on the equatorial plane as follows:

$$V = V_+ = \frac{\epsilon Q}{r} + \sqrt{\left(1 - \frac{2M}{r} + \frac{Q^2}{r^2}\right) \left(\mu^2 + \frac{L^2}{r^2}\right)}. \quad (4.14)$$

- massless charged particle:

For a massless charged particle, we have

$$V = \frac{\epsilon Q}{r} + \sqrt{\left(1 - \frac{2M}{r} + \frac{Q^2}{r^2}\right) \frac{L^2}{r^2}}, \quad (4.15)$$

(1) Choosing $\epsilon = 5$ and $L = 2$, we find that $-\epsilon Q = -3 < L$. The graph of the potential function is shown in Fig. 6. From this figure, it is evident that there exists an unstable photon circular orbit between r_h and infinity, which is consistent with the result (4.4).

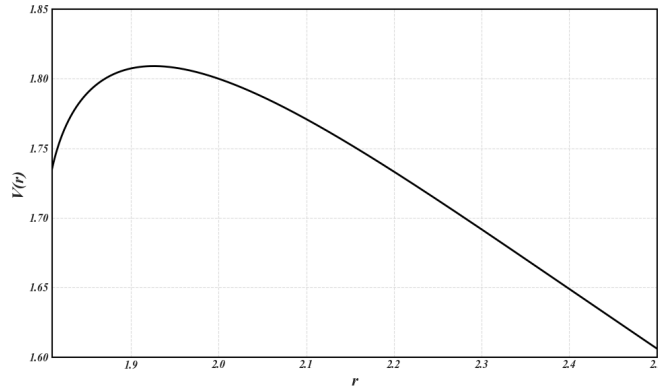


FIG. 6: For $\epsilon = 5$ and $L = 2$, there is an unstable null circular orbits.

(2) Choosing $\epsilon = -\frac{10}{3}$ and $L = 2$, then we have $-\epsilon Q = 2 = L$. The graph of the potential function is shown in Fig. 7. From this figure, it is evident that there are no null circular orbits between r_h and infinity, which is consistent with the result (4.5).

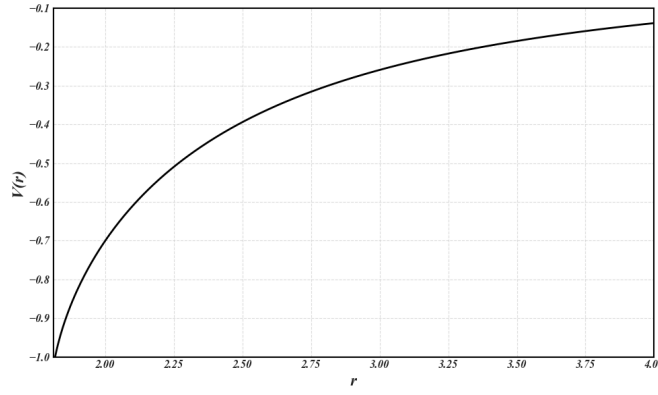


FIG. 7: For $\epsilon = -\frac{10}{3}$ and $L = 2$, there are no null circular orbits.

(3) Choosing $\epsilon = -5$ and $L = 2$, then we have $-\epsilon Q = 3 > L$. The graph of the potential function is given in Fig. 8. From this figure, it is evident that there are no null circular orbits between r_h and infinity, which is consistent with the result (4.5).

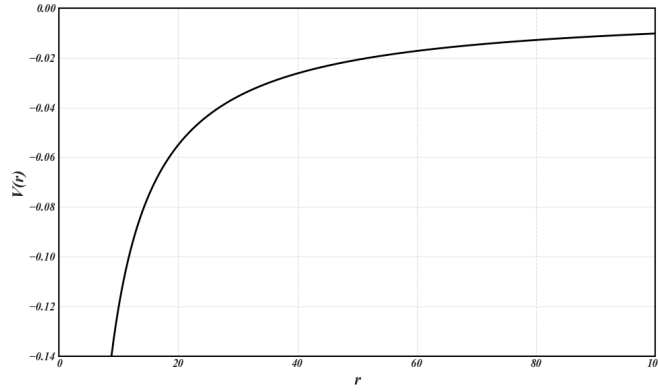


FIG. 8: For $\epsilon = -5$ and $L = 2$, There are no null circular orbits.

- massive charged particle:

For a massive charged particle, we have

$$V = \frac{\epsilon Q}{r} + \sqrt{\left(1 - \frac{2M}{r} + \frac{Q^2}{r^2}\right) \left(1 + \frac{L^2}{r^2}\right)}, \quad (4.16)$$

(1) Choosing $\epsilon = 2$ and $L = 2$, we find that $\epsilon Q = 1.2 > M = 1$. The graph of the potential function is shown in Fig. 9. From this figure, it is evident that there is one unstable timelike circular orbit between r_h and infinity, which is consistent with the result (4.10).

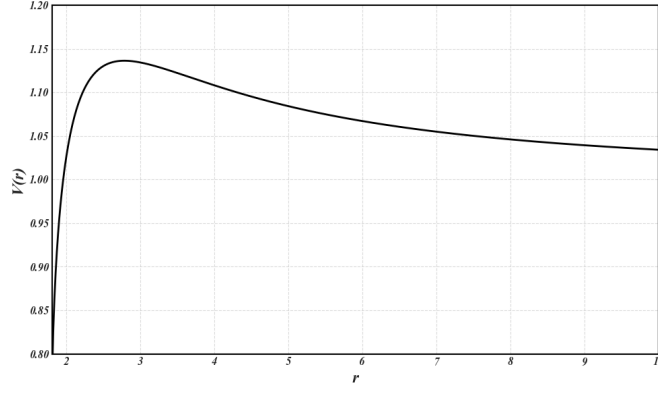


FIG. 9: For $\epsilon = 2$ and $L = 2$, there is one unstable timelike circular orbits.

(2) Choosing $\epsilon = \frac{5}{3}$ and $L = 2$, we find that $\epsilon Q = 1 = M$. The graph of the potential function is shown in Fig. 10. From this figure, it is evident that there is one unstable timelike circular orbit between r_h and infinity, which is consistent with the result (4.10).

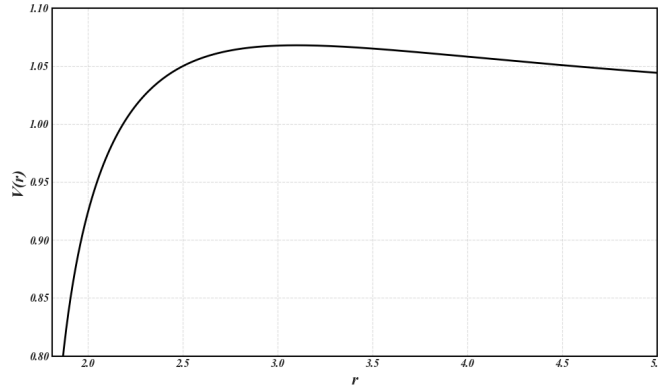


FIG. 10: For $\epsilon = \frac{5}{3}$ and $L = 2$, there is one unstable timelike circular orbits.

(3) Choosing $\epsilon = \frac{7}{6}$ and $L = 2$, we find that $\epsilon Q = 0.7 < M$. The graph of the potential function is shown in Fig. 11. From this figure, it is evident that there is one unstable timelike circular orbit and one stable timelike circular orbit between r_h and infinity, which is consistent with the result (4.9).

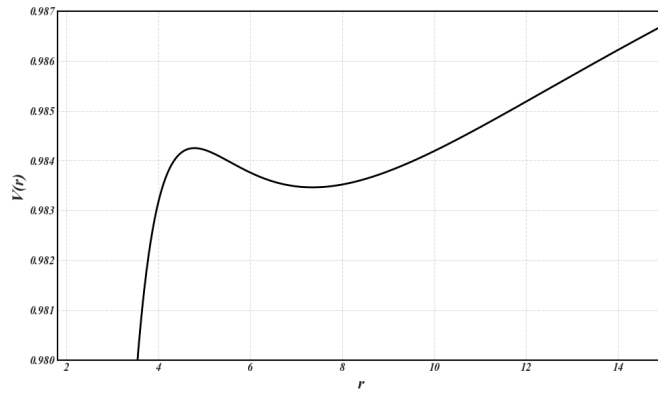


FIG. 11: For $\epsilon = \frac{7}{6}$ and $L = 2$, there is one unstable timelike circular orbits and one stable timelike circular orbits.

(4) Choosing $\epsilon = 1$ and $L = 2$, we find that $\epsilon Q = 0.6 < M$. The graph of the potential function is shown in Fig. 12. From this figure, it is evident that there are no timelike circular orbits between r_h and infinity, which is consistent with the result (4.9).

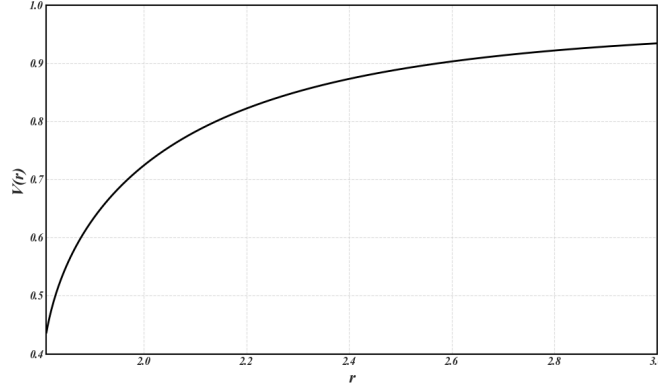


FIG. 12: For $\epsilon = 1$ and $L = 2$, there are no timelike circular orbits.

B. Asymptotically AdS black holes

An asymptotically AdS black hole exhibits the following asymptotic behavior:

$$\begin{aligned} f(r) &\sim \frac{r^2}{l^2} + 1 - \frac{2M}{r} + \mathcal{O}\left(\frac{1}{r^2}\right), \\ g(r) &\sim \frac{r^2}{l^2} + 1 - \frac{2M}{r} + \mathcal{O}\left(\frac{1}{r^2}\right), \\ h(r) &\sim r^2, \end{aligned} \tag{4.17}$$

where l is the AdS radius. For $r_h < r < \infty$, the function $f(r)$ exhibits the behavior shown in Fig. 13, and $f'(r) > 0$ at r_h . Note that these asymptotic behaviors only modify the boundary condition at $r \rightarrow \infty$, so the calculation along l_2, l_3 and l_4 is the same as the asymptotically flat case.

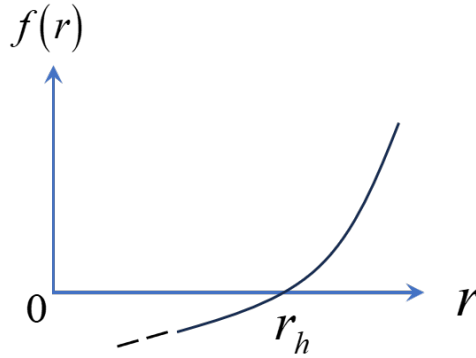


FIG. 13: The behavior of $f(r)$ in asymptotically flat black hole, and $f'(r) > 0$ at r_h .

The contour we chosen in asymptotically AdS spacetimes is shown in Fig. 14, which is same as asymptotically flat spacetimes. Therefore, the same boundary behavior will yield the same results.

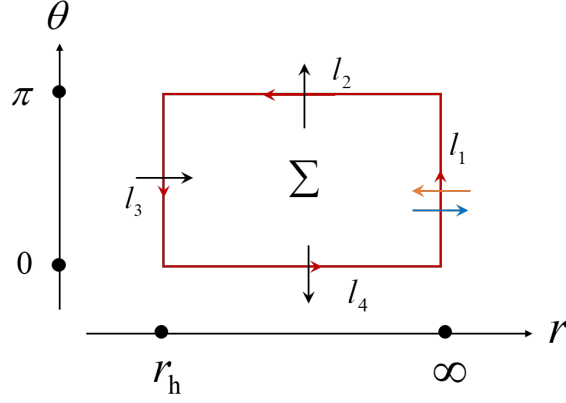


FIG. 14: The representation of the contour $C = \sum_i \cup l_i$ (which encloses Σ) on the (r, θ) plane. The curve C has a positive orientation marked with the red arrows. The black, blue and yellow arrows indicate the approximate direction of the vector ϕ along the boundaries.

1. charged massless particles

When $r \rightarrow \infty$, we have a finite l , and

$$\phi_{l_1}^r(r \rightarrow \infty) = -\frac{\epsilon Q}{rl} - \frac{L}{r^2} \quad (4.18)$$

on the equatorial plane.

If $\epsilon Q \geq 0$, one has $\phi_{l_1}^r(r \rightarrow \infty) < 0$. Following the results in asymptotically flat spacetimes, the total topological number is

$$W = -1, \quad (4.19)$$

which means that there will always be at least one unstable null circular orbit outside the event horizon in asymptotically AdS black holes.

If $\epsilon Q < 0$, one has $\phi_{l_1}^r(r \rightarrow \infty) > 0$. Following the results in asymptotically flat spacetimes, the total topological number is

$$W = 0, \quad (4.20)$$

which means that if null circular orbits exist in asymptotically AdS black holes, they must occur in pairs, with one being stable and the other unstable.

2. charged massive particles

When $r \rightarrow \infty$, we have a finite l , and

$$\phi_{l_1}^r(r \rightarrow \infty) = \frac{r}{l^2}, \quad (4.21)$$

Thus, we will always have $\phi_{l_1}^r(r \rightarrow \infty) > 0$. Following the results in asymptotically flat spacetimes, the total topological charge is

$$Q = 0, \quad (4.22)$$

which means that if timelike circular orbits (TCOs) exist in asymptotically AdS spacetime, they must occur in pairs, with one being stable and the other unstable.

3. RN-AdS black hole

Here, we use Reissner-Nordström Anti-de Sitter (RN-AdS) black holes as an example to verify the above conclusions. For a RN-AdS black hole, the functions $f(r)$, $g(r)$ and $h(r)$ in (2.1) are given by

$$f(r) = g(r) = 1 - \frac{2M}{r} + \frac{Q^2}{r^2} + \frac{r^2}{l^2}, \quad h(r) = r^2. \quad (4.23)$$

The associated electromagnetic potential is

$$A = -\frac{Q}{r} dt. \quad (4.24)$$

Below, we set $M = 1$, $Q = 0.6$ and $l = 100$. The graph of the function $f(r)$ is shown in Fig. 15, with $r_- = 0.2$, $r_+ = 1.79934$.

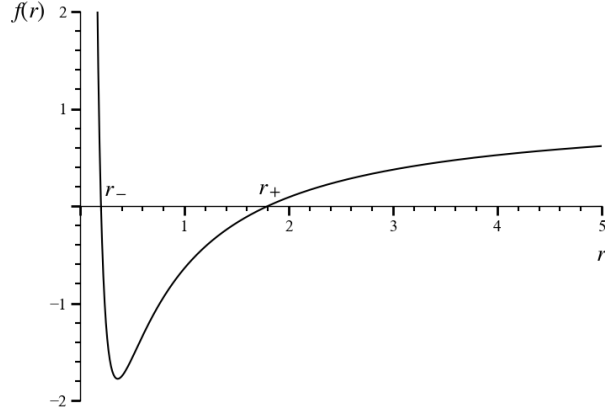


FIG. 15: The behavior of $f(r)$ in RN-AdS black hole. At r_- , one has $f'(r) < 0$; at r_+ , one has $f'(r) < 0$.

In the region between r_- and r_+ , there are no circular orbits. Therefore, we focus on the case where $r > r_+$.

- massless charged particle:

For a massless charged particle, we have

$$V = \frac{\epsilon Q}{r} + \sqrt{\left(1 - \frac{2M}{r} + \frac{Q^2}{r^2} + \frac{r^2}{l^2}\right) \frac{L^2}{r^2}}, \quad (4.25)$$

(1) Choosing $\epsilon = \frac{1}{6}$ and $L = 2$, we find that $\epsilon Q = 0.1 > 0$. The graph of the potential function is shown in Fig. 16. From this figure, it is evident that there exists one unstable photon circular orbit between r_h and infinity, which is consistent with the result (4.19).

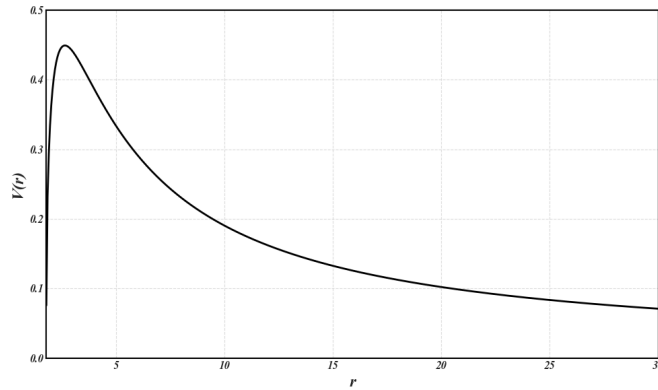


FIG. 16: For $\epsilon = \frac{1}{6}$ and $L = 2$, there is one unstable null circular orbits.

(2) Choosing $\epsilon = 0$ and $L = 2$, then we have $\epsilon Q = 0$. The graph of the potential function is shown in Fig. 17. From this figure, it is evident that there exists one unstable photon circular orbit between r_h and infinity, which is consistent with the result (4.19).

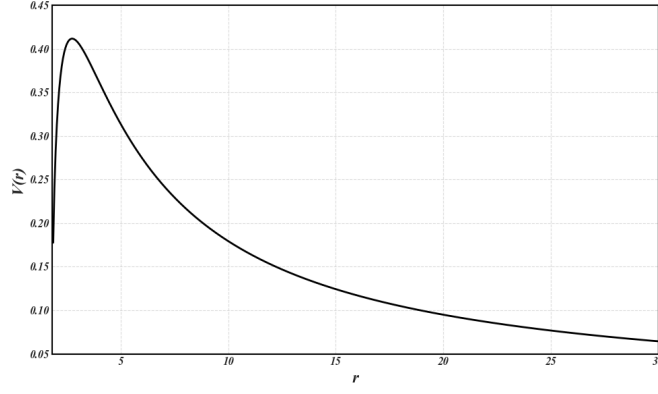


FIG. 17: For $\epsilon = 0$ and $L = 2$, there is one unstable null circular orbits.

(3) Choosing $\epsilon = -\frac{1}{6}$ and $L = 2$, we find that $\epsilon Q = -0.1 < 0$. The graph of the potential function is shown in Fig. 18. From this figure, it is evident that there are no null circular orbits between r_h and infinity, which is consistent with the result (4.20).

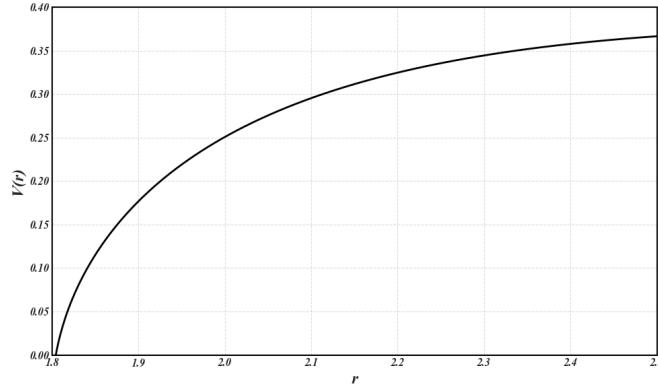


FIG. 18: For $\epsilon = -\frac{1}{6}$ and $L = 2$, there are no null circular orbits.

- massive charged particle:

For a massive charged particle, we have

$$V = \frac{\epsilon Q}{r} + \sqrt{\left(1 - \frac{2M}{r} + \frac{Q^2}{r^2} + \frac{r^2}{l^2}\right) \left(1 + \frac{L^2}{r^2}\right)}, \quad (4.26)$$

(1) Choosing $\epsilon = \frac{5}{3}$ and $L = 2$, we find that $\epsilon Q = 1$. The graph of the potential function is shown in Fig. 19. From this figure, it is evident that there exists one unstable timelike circular orbit and one stable timelike circular orbit between r_h and infinity, which is consistent with the result (4.22).

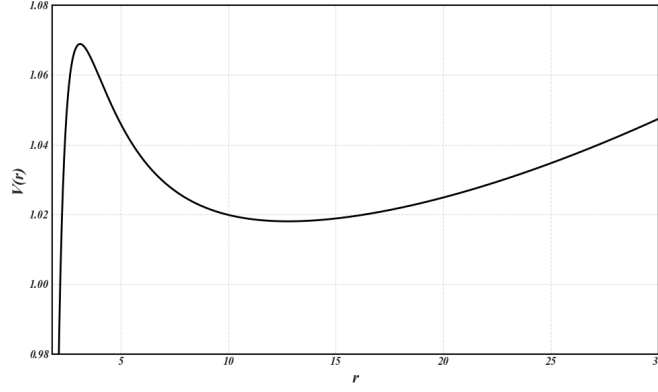


FIG. 19: For $\epsilon = \frac{5}{3}$ and $L = 2$, there are one unstable timelike circular orbit and one stable timelike circular orbit.

(2) Choosing $\epsilon = -\frac{5}{3}$ and $L = 2$, we find that $\epsilon Q = -1$. The graph of the potential function is shown in Fig. 20. From this figure, it is evident that there are no timelike circular orbits between r_h and infinity, which is consistent with the result (4.22).

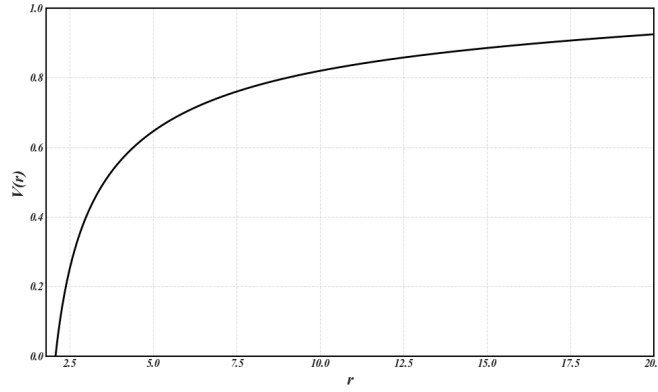


FIG. 20: For $\epsilon = -\frac{5}{3}$ and $L = 2$, there are no timelike circular orbits.

C. Asymptotically dS black holes

Now we turn to the asymptotically dS black hole case, which exhibits the following asymptotic behavior at large r

$$f(r) \sim -\frac{r^2}{l^2} + 1 - \frac{2M}{r} + \mathcal{O}\left(\frac{1}{r^2}\right), \quad (4.27)$$

$$g(r) \sim -\frac{r^2}{l^2} + 1 - \frac{2M}{r} + \mathcal{O}\left(\frac{1}{r^2}\right), \quad (4.28)$$

$$h(r) \sim r^2, \quad (4.29)$$

Unlike the asymptotically flat and AdS cases, besides the black hole horizon, the spacetime admits a cosmological horizon with radius $r_c > r_h$, which is also a root of $g(r_c) = f(r_c) = 0$. Therefore, for this case, we restrict our consideration to $r_h \leq r \leq r_c$. The behavior of $f(r)$ within $r_h \leq r \leq r_c$ is shown in Fig. 21, which corresponds exactly to situation (b) in Fig. 2.

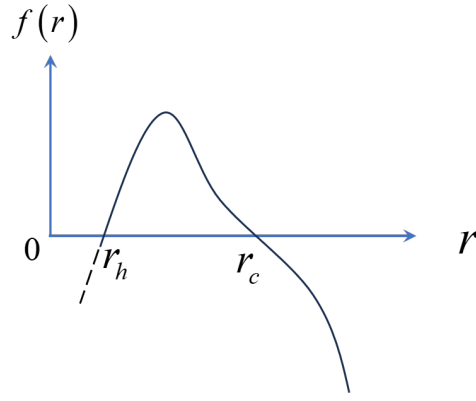


FIG. 21: The behavior of $f(r)$ in asymptotically dS black hole. One has $f'(r) < 0$ at r_h and $f'(r) > 0$ at r_c . Here, r_h denotes the outermost black hole horizon, while r_c represents the cosmological horizon.

Thus, one can easily derive

$$W = -1 \quad (4.30)$$

for both charged massless particles and charged massive particles. This implies that there will always be at least one unstable null circular orbit and one unstable timelike circular orbit between r_h and r_c in asymptotically dS black hole.

1. RN-dS black hole

Here, we use Reissner-Nordström de Sitter black holes (RN-dS) as an example to verify the above conclusions. For a RN-dS black hole, the functions $f(r)$, $g(r)$ and $h(r)$ in (2.1) are given by

$$f(r) = g(r) = 1 - \frac{2M}{r} + \frac{Q^2}{r^2} - \frac{r^2}{l^2}, \quad h(r) = r^2. \quad (4.31)$$

The associated electromagnetic potential is

$$A = -\frac{Q}{r} dt. \quad (4.32)$$

Below, we set $M = 1$, $Q = 0.6$ and $l = 10$. The graph of the function $f(r)$ is shown in Fig. 22, with $r_- = 0.3674$, $r_+ = 1.6946$ and $r_c = 8.83985$. In the region between r_- and r_+ , there are no circular orbits. Therefore, we focus on the case where $r_+ < r < r_c$.

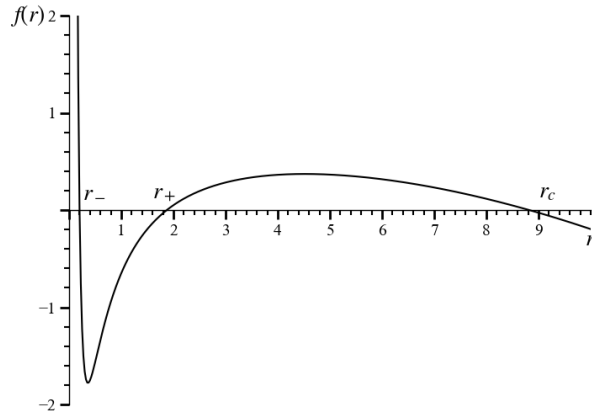


FIG. 22: The behavior of $f(r)$ in RN black hole, and one have $f'(r) > 0$ at r_+ and $f'(r) < 0$ at r_c .

- massless charged particle:

For a massless charged particle, we have

$$V = \frac{\epsilon Q}{r} + \sqrt{\left(1 - \frac{2M}{r} + \frac{Q^2}{r^2} - \frac{r^2}{l^2}\right) \frac{L^2}{r^2}}, \quad (4.33)$$

(1) Choosing $\epsilon = 1$ and $L = 2$, we find that $\epsilon Q = 0.6$. The graph of the potential function is shown in Fig. 23. From this figure, it is evident that there is an unstable null circular orbit between r_h and r_c , which is consistent with the result (4.30).

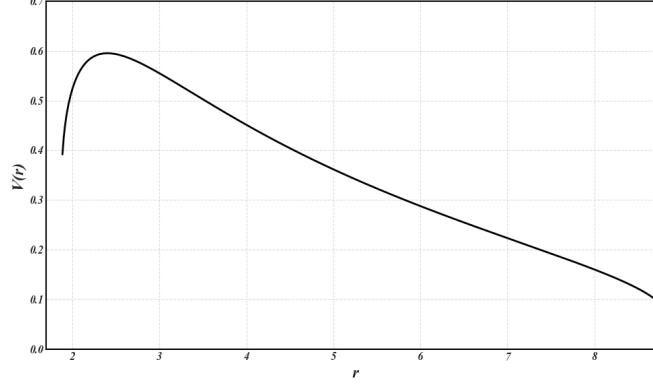


FIG. 23: For $\epsilon = 1$ and $L = 2$, there is an unstable null circular orbit.

(2) Choosing $\epsilon = -1$ and $L = 2$, we find that $\epsilon Q = -0.6$. The graph of the potential function is shown in Fig.24. From this figure, it is evident that there is an unstable null circular orbit between r_h and r_c , which is consistent with the result (4.30).

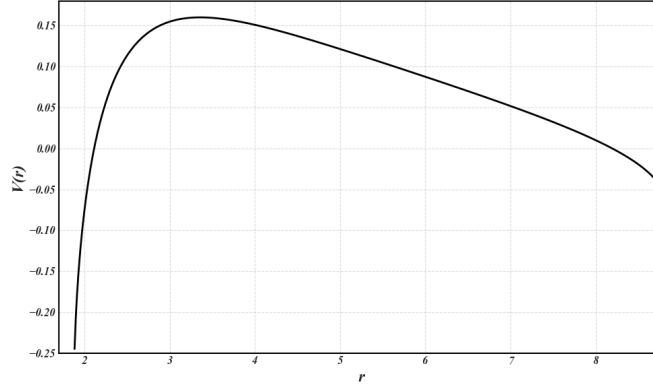


FIG. 24: For $\epsilon = -1$ and $L = 2$, there is an unstable null circular orbit.

- massive charged particle:

For a massive charged particle, we have

$$V = \frac{\epsilon Q}{r} + \sqrt{\left(1 - \frac{2M}{r} + \frac{Q^2}{r^2} - \frac{r^2}{l^2}\right) \left(1 + \frac{L^2}{r^2}\right)}, \quad (4.34)$$

(1) Choosing $\epsilon = 1$ and $L = 2$, we find that $\epsilon Q = 0.6$. The graph of the potential function is shown in Fig. 25. From this figure, it is evident that there is an unstable TCO between r_h and r_c , which is consistent with the result (4.30).

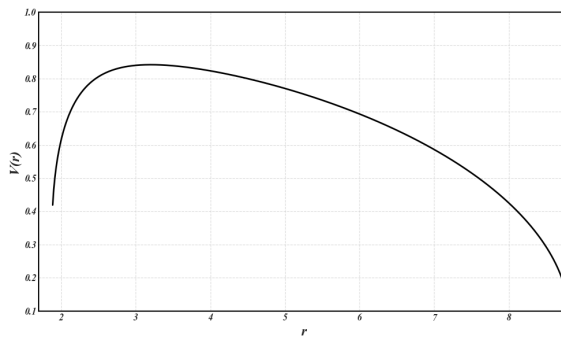


FIG. 25: For $\epsilon = 1$ and $L = 2$, there is an unstable TCO.

(2) Choosing $\epsilon = -1$ and $L = 2$, we find that $\epsilon Q = -0.6$. The graph of the potential function is shown in Fig.26. From this figure, it is evident that there is an unstable TCO between r_h and r_c , which is consistent with the result (4.30).

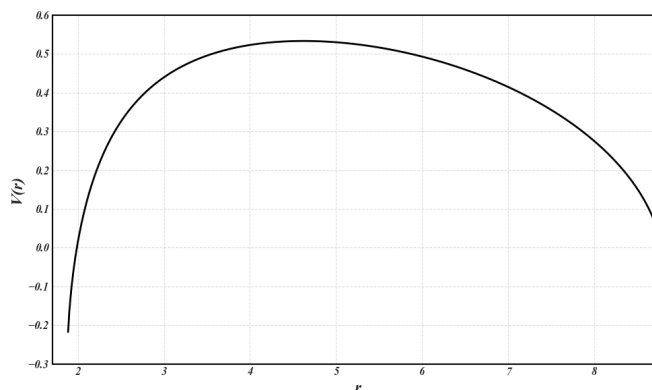


FIG. 26: For $\epsilon = -1$ and $L = 2$, there is an unstable TCO.

V. CONCLUSIONS AND DISCUSSIONS

In this study, we have systematically investigated the topological properties of circular orbits for charged test particles in asymptotically flat, anti-de Sitter (AdS), and de Sitter (dS) black holes with multiple horizons. By employing a topological approach based on vector field analysis and winding number calculations, we have uncovered the influence of particle charge and spacetime asymptotic behavior on the existence and stability of both timelike and null circular orbits. Our findings are further validated through explicit examples of Reissner-Nordström (RN), RN-AdS, and RN-dS black holes. The key conclusions are summarized in Fig. 27:

- **Multi-horizon black holes:** For black holes with multiple horizons, if circular orbits exist between two neighboring horizons (Case (a) in Fig. 2), there must always exist at least one unstable null circular orbit and one unstable timelike circular orbit. Conversely, regions where $f(r) < 0$ (Case (b)) forbid such orbits entirely.
- **Asymptotically flat black holes:** For null orbits, the topological number W depends on the charge (ϵQ) and angular momentum (L) of the charged particle. When $-\epsilon Q < L$, $W = -1$, indicating there exists at least one unstable orbit. If $-\epsilon Q \geq L$, $W = 0$, implying paired orbits (one stable, one unstable) or none.
For TCOs, the black hole mass (M) and the charge (ϵQ) determine W . When $M > \epsilon Q$, $W = 0$ implying paired TCOs (one stable, one unstable) or none. If $M \leq \epsilon Q$, $W = -1$, indicating there exists at least one unstable TCO.
- **Asymptotically AdS black holes:** Null circular orbits exhibit $W = -1$ for $\epsilon Q \geq 0$, guaranteeing an unstable orbit. For $\epsilon Q < 0$, $W = 0$, permitting paired orbits. TCOs universally yield $W = 0$, requiring paired orbits when they exist, independent of particle charge.
- **Asymptotically dS black holes:** Between the outermost event horizon (r_h) and cosmological horizon (r_c), both null and timelike circular orbits always have at least one unstable circular orbit ($W = -1$), regardless of particle charge.

	Null circular orbits	TCOs
Neighboring horizons	<i>Case (a):</i> $W = -1$ <i>Case (b):</i> <i>Forbidden</i>	<i>Case (a):</i> $W = -1$ <i>Case (b):</i> <i>Forbidden</i>
Asymptotically flat black hole (outsider the outer horizon)	$-\epsilon Q < L, \quad W = -1;$ $-\epsilon Q \geq L, \quad W = 0.$	$M > \epsilon Q, \quad W = 0;$ $M \leq \epsilon Q, \quad W = -1.$
Asymptotically AdS black hole (outsider the outer horizon)	$\epsilon Q \geq 0, \quad W = -1;$ $\epsilon Q < 0, \quad W = 0.$	$W = 0$
Asymptotically dS black hole (Between r_h and r_c)	$W = -1$	$W = -1$

FIG. 27: The impact of black hole asymptotic behavior and particle charge on the topological properties of circular orbits in spacetime.

These results highlight the critical role of spacetime asymptotics and particle charge in shaping the topological landscape of circular orbits. Notably, the charge of a particle introduces additional constraints on orbit stability, distinguishing this work from previous studies focused on neutral particles.

While our analysis assumes static, spherically symmetric black holes, rotating black holes may exhibit richer topological structures due to frame-dragging effects. However, based on Ref. [3], we conjecture that the total topological charge for rotating black holes with flat, AdS, or dS asymptotics will align with our findings, a hypothesis warranting rigorous verification.

Appendix A: The case of $V=V_-$

For the case of $V = V_-$, following the previous calculation, one can easily get the topological properties of circular orbits, and the results are shown in Fig.28. Below, we summarize the main results:

- **Multi-horizon black holes:** For black holes with multiple horizons, if circular orbits exist between two neighboring horizons (Case (a) in Fig.2), there must always be at least one stable null circular orbit and one stable timelike circular orbit. Conversely, regions where $f(r) < 0$ (Case (b)) forbid such orbits entirely.
- **Asymptotically flat black holes:** For null orbits, the topological number W depends on the charge ϵQ and specific angular momentum L . When $\epsilon Q < L$, $W = +1$, indicating there exists at least one stable orbit. If $\epsilon Q \geq L$, $W = 0$, implying paired orbits (one stable, one unstable) or none.
For TCOs, the black hole mass M and charge ϵQ determine W . When $M > -\epsilon Q$, $W = 0$ allowing paired orbits (one stable, one unstable) or none. If $M \leq -\epsilon Q$, $W = +1$, indicating there exists at least one stable orbit. These results are consistent with [12].
- **Asymptotically AdS black holes:** Null circular orbits exhibit $W = +1$ for $\epsilon Q \leq 0$, guaranteeing an stable orbit. For $\epsilon Q > 0$, $W = 0$, permitting paired orbits. TCOs universally yield $W = 0$, requiring paired orbits when they exist, independent of particle charge.
- **Asymptotically dS black holes:** Between the event horizon (r_h) and cosmological horizon (r_c), both null and timelike circular orbits always have at least one stable circular orbit ($W = +1$), regardless of particle charge.

	Null circular orbits	TCOs
Neighboring horizons	<i>Case (a)</i> : $W = +1$ <i>Case (b)</i> : <i>Forbidden</i>	<i>Case (a)</i> : $W = +1$ <i>Case (b)</i> : <i>Forbidden</i>
Asymptotically flat black hole (outsider the outer horizon)	$\epsilon Q < L, W = +1;$ $\epsilon Q \geq L, W = 0.$	$M > -\epsilon Q, W = 0;$ $M \leq -\epsilon Q, W = +1.$
Asymptotically AdS black hole (outsider the outer horizon)	$\epsilon Q > 0, W = 0;$ $\epsilon Q \leq 0, W = +1.$	$W = 0$
Asymptotically dS black hole (Between r_h and r_c)	$W = +1$	$W = +1$

FIG. 28: For $V=V_-$, topology of circular orbits for charged particles in spacetime.

-
- [1] P. V. P. Cunha, E. Berti and C. A. R. Herdeiro, Phys. Rev. Lett. **119**, no.25, 251102 (2017) doi:10.1103/PhysRevLett.119.251102 [arXiv:1708.04211 [gr-qc]].
- [2] S. Hod, Phys. Lett. B **776**, 1-4 (2018) doi:10.1016/j.physletb.2017.11.021 [arXiv:1710.00836 [gr-qc]].
- [3] P. V. P. Cunha and C. A. R. Herdeiro, Phys. Rev. Lett. **124**, no.18, 181101 (2020) doi:10.1103/PhysRevLett.124.181101 [arXiv:2003.06445 [gr-qc]].
- [4] Y. S. Duan and M. L. Ge, Sci. Sin. **9**, no.11, 1072 (1979) doi:10.1142/9789813237278.0001
- [5] Y. Duan, SLAC-PUB-3301.
- [6] S. W. Wei, Phys. Rev. D **102**, no.6, 064039 (2020) doi:10.1103/PhysRevD.102.064039 [arXiv:2006.02112 [gr-qc]].
- [7] S. W. Wei and Y. X. Liu, Phys. Rev. D **105**, no.10, 104003 (2022) doi:10.1103/PhysRevD.105.104003 [arXiv:2112.01706 [gr-qc]].
- [8] S. W. Wei, Y. X. Liu and R. B. Mann, Phys. Rev. Lett. **129**, no.19, 191101 (2022) doi:10.1103/PhysRevLett.129.191101 [arXiv:2208.01932 [gr-qc]].
- [9] S. W. Wei and Y. X. Liu, Phys. Rev. D **107**, no.6, 064006 (2023) doi:10.1103/PhysRevD.107.064006 [arXiv:2207.08397 [gr-qc]].
- [10] X. Ye and S. W. Wei, JCAP **07**, 049 (2023) doi:10.1088/1475-7516/2023/07/049 [arXiv:2301.04786 [gr-qc]].
- [11] M. U. Shahzad, N. Alessa, A. Mehmood and M. Z. Ashraf, Nucl. Phys. B **1010**, 116749 (2025) doi:10.1016/j.nuclphysb.2024.116749
- [12] X. Ye and S. W. Wei, Class. Quant. Grav. **42**, no.2, 025020 (2025) doi:10.1088/1361-6382/ad9f14 [arXiv:2406.13270 [gr-qc]].
- [13] Y. Q. Lei and X. H. Ge, Phys. Rev. D **105**, no.8, 084011 (2022) doi:10.1103/PhysRevD.105.084011 [arXiv:2111.06089 [hep-th]].
- [14] D. Pugliese, H. Quevedo and R. Ruffini, Phys. Rev. D **83**, 104052 (2011) doi:10.1103/PhysRevD.83.104052 [arXiv:1103.1807 [gr-qc]].
- [15] Y. K. Lim, Phys. Rev. D **91**, no.2, 024048 (2015) doi:10.1103/PhysRevD.91.024048 [arXiv:1502.00722 [gr-qc]].
- [16] N. Kurbonov, J. Rayimbaev, M. Alloqulov, M. Zahid, F. Abdulxamidov, A. Abdujabbarov and M. Kurbanova, Eur. Phys. J. C **83**, no.6, 506 (2023) doi:10.1140/epjc/s10052-023-11691-9